The Astrophysical Journal, 620:L35–L38, 2005 February 10

THE DETECTION OF NONTHERMAL RADIO CONTINUUM SPOKES AND THE STUDY OF STAR FORMATION IN THE CARTWHEEL

Y. D. Mayya,[1] D. Bizyaev,[2,3,4] R. Romano,[1] J. A. Garcia-Barreto,[5] and E. I. Vorobyov[6]

Received 2004 October 21; accepted 2004 December 23; published 2005 January 17

ABSTRACT

New sensitive Very Large Array 20 cm continuum observations of the Cartwheel, the prototypical collisional ring galaxy, were carried out with the principal aim of tracing supernova remnants that are expected to lie in the wake of the expanding ring and in the ring itself. We detect predominantly nonthermal radio continuum emission from regions associated with 13 ring H II complexes. The emission interior to the ring is confined to structures that resemble spokes of the wheel. The spokes start near bright H II complexes and extend to around 6″ (4 kpc) inward in the direction of the geometrical center of the ring. There is no apparent positional coincidence between the radio continuum and optical spokes. Radial distribution of intensity along the spokes suggests that the past star formation rate (SFR) in the Cartwheel was much lower than the current SFR. New Hα observations were used to revise the current SFR in the Cartwheel. The revised value is 18 $M_{\odot}$ yr^{-1}, which is a factor of 4 lower than the value reported previously but is in good agreement with the SFR estimated from far-infrared luminosity. About 30% of the observed 20 cm continuum nonthermal emission seems to originate in processes that are not related to star formation. Revised SFR in the Cartwheel is comparable to that in the rest of the ring galaxies.

Subject headings: galaxies: individual (Cartwheel) — galaxies: interactions

Online material: color figure

1. INTRODUCTION

Ring galaxies represent a class of colliding galaxies in which nearly symmetrical density waves are driven into a disk as a result of an almost bull's-eye collision with a compact galaxy (Lynds & Toomre 1976; Theys & Spiegel 1977). Hydrodynamical simulations reproduce some of the basic features observed in ring galaxies, such as rings or crescent-shaped structures (Hernquist & Weil 1993; Gerber et al. 1996). Expanding density waves trigger star formation (SF), and hence a star-forming ring is expected to form in ring galaxies. The star-forming ring propagates outward with time, leaving behind an evolved stellar population in its wake. Tracers of massive short-lived stars (e.g., Hα emission) are expected to delineate the present position of the wave, while tracers of the remnants of massive stars (e.g., nonthermal radio continuum) are expected to illuminate the regions in the wake of the expanding wave. Initial gas density distribution and the velocity of the wave would determine the shapes of the radial intensity profiles in the tracers of the young and old components (Korchagin et al. 2001).

The Cartwheel is among the biggest known ring galaxies, in both angular and linear size, and is considered to be the prototype of a ring galaxy. At a distance of 137 Mpc (H_0 = 65 km s^{-1} Mpc^{-1}), its angular size of 72″ corresponds to a linear diameter of 48 kpc. The entire population of bright H II regions lies in the outer ring, with more than 80% of the current SF occurring in a few H II complexes in the southern sector of the ring (Higdon 1995, hereafter H95). There are, however, a few faint regions inside (Amram et al. 1998). H95 derived a star formation rate (SFR) of 67 $M_{\odot}$ yr^{-1} (159 $M_{\odot}$ yr^{-1} for the H_0 adopted in this work), based on Hα flux, which is almost an order of magnitude higher than that derived from far-infrared (FIR) flux. Some of this discrepancy is probably due to problems in the H95 calibration of Hα fluxes (J. L. Higdon 2000, private communication).

We have carried out sensitive 20 cm radio continuum (RC) observations using the Very Large Array (VLA)[7] with the goal of detecting nonthermal emission in the wake of the wave. We also carried out new Hα observations in order to resolve the discrepancy between the SFRs derived from Hα and FIR luminosity. We present details of the new observations in § 2. In § 3, we describe the observed radio structures and also discuss the SFRs derived from Hα, FIR, and RC fluxes. In § 4, we discuss the results obtained from these new observations from the context of expanding wave models.

2. NEW RC AND Hα OBSERVATIONS

RC observations at 20 cm were carried out with the BnA configuration of the VLA during 2002 May and June, spread over seven runs totaling 35 hr of integration time. The flux scale, antenna gain, and phase constants were calibrated using observations of standards 0137+331 (16.32 Jy at 1.38 GHz) and 0025−260 (8.70 Jy at 1.38 GHz). Data for each run were calibrated before combining them to produce the final map. The final cleaned and self-calibrated maps have almost a circular beam of FWHM of 3.″3 × 3.″0 (P.A. = 36°). Several maps with different weight parameters and deconvolved beam sizes were obtained. Some maps were only cleaned, and others were

[1] Instituto Nacional de Astrofísica, Optica y Electronica, Luis Enrique Erro 1, Tonantzintla, CP 72840 Puebla, Mexico.

[2] Department of Physics, University of Texas at El Paso, 500 West University Avenue, El Paso, TX 79968.

[3] Sternberg Astronomical Institute, 13, Universitetsky Prospekt, Moscow 119899, Russia.

[4] Isaac Newton Institute of Chile (Moscow branch), 48 Pyatnitskaya Str., Moscow 119017, Russia.

[5] Insituto de Astronómia, Universidad Nacional Autonoma de México, Apdo. Postal 70-264, Cd. Unversitaria 04510 México DF, Mexico.

[6] Institute of Physics, Stachki 194, Rostov-on-Don, Russia; and Department of Physics and Astronomy, University of Western Ontario, London, ON N6A 3K7, Canada.

[7] The VLA is part of the National Radio Astronomy Observatory, which is a facility of the National Science Foundation operated under cooperate agreement by Associated Universities, Inc.

TABLE 1
FIR, Hα, AND 20 cm FLUXES AND SFRs

Quantity	FIR	Hα	20 cm
Flux	-13.23 ± 0.12[a]	-12.40 ± 0.04[b]	12.8 ± 0.5[c]
log luminosity	10.50 $L_\odot$	41.95 ergs s^{-1}	29.46 W Hz^{-1}
SFR ($M_\odot$ yr^{-1}):			
$A_v = 0.0$	17.71	7.91	29.13
$A_v = 1.2$	17.71	18.13	27.67
$A_v = 1.7$	17.71	25.60	26.61

[a] Logarithmic flux in units of W m^{-2}.
[b] Logarithmic flux in units of ergs s^{-1} cm^{-2}.
[c] In units of millijanskys.

the result of several iterations of self-calibration with different restoring beam sizes. The rms or σ noise of our final image is 30 μJy $beam^{-1}$, which is an improvement by around a factor of 4 over previous observations (Higdon 1996, hereafter H96). Although some of the radio structures that we discuss here are at the nominal 3 σ limit or just below it, we believe that these structures are true because of their presence in various trial maps that we had produced during the reduction process.

New Hα CCD imaging observations were carried out during one photometric night (2003 September 30) at the McDonald observatory (Texas) with a 30″ telescope. We used three interference filters: 6700/123, 6560/100, and 6670/82, designated so for their central wavelengths and widths, both in units of Å. The first one intercepts the redshifted Hα line from the galaxy (6761 Å), and the other two filters facilitate subtraction of the continuum flux entering the Hα filter. We took two exposures of the galaxy (totaling 35 minutes) as well as the standard stars in each filter. The exposures of the galaxy were bracketed in time and zenith distance by the calibration stars LTT 377 and LTT 1020 (Hamuy et al. 1994).

The measured total RC and Hα fluxes, along with errors on our measurements, are given in Table 1. Our 20 cm flux is in good agreement with the value published by H96 (11.5 mJy). Hα fluxes in this table have been corrected for 10% contribution from [N II] lines (Fosbury & Hawarden 1977) and galactic extinction (2.6%). Our value is around 4 times lower than that given by H95.

We used our new total flux to calibrate an excellent quality Hα image (seeing FWHM = 0.″8) that is available at the Canada-France-Hawaii Telescope data archive. Figure 1 shows the 20 cm contours superposed on gray-scale representation of an Hα image that is smoothed to the resolution of the radio image, and full-resolution *Hubble Space Telescope* (*HST*) *B*-band image in panels *a* and *b*, respectively. In the following section we give a description of the different observed features.

3. RC MORPHOLOGY AND THE NATURE OF RADIO EMISSION

It can be seen in Figure 1 that the RC morphology of the Cartwheel resembles very much the morphology of the ring in Hα emission. Radio emission is detected from at least 13 H II complexes. These complexes are among the brightest 15 in Hα emission (brighter than 8.31×10^{-15} ergs cm^{-2} s^{-1}). The two nondetected sources (CW-6 and CW-29 of H95) are among the regions with the highest Hα equivalent widths, suggesting that they are most likely too young to turn on nonthermal RC emission. Faint emission is also detected at the nuclear position (Fig. 1, *cross*). In the bright southern part of the ring, the RC image shows at least seven finger-like structures that seem to originate from parts of the ring near bright H II regions and point radially inward to the geometrical center of the ring, giving the appearance of spokes of the wheel. The most prominent spoke originates from close to CW-17, the brightest H II region in the Cartwheel. This is the only spoke that had been detected in previous RC images (H96). The spoke originating near CW-20 crosses the ring, although with a slight change in the direction. Interestingly, the hyperluminous X-ray source reported by Gao et al. (2003) coincides with this region.

Are the RC spokes related to their optical counterparts? The

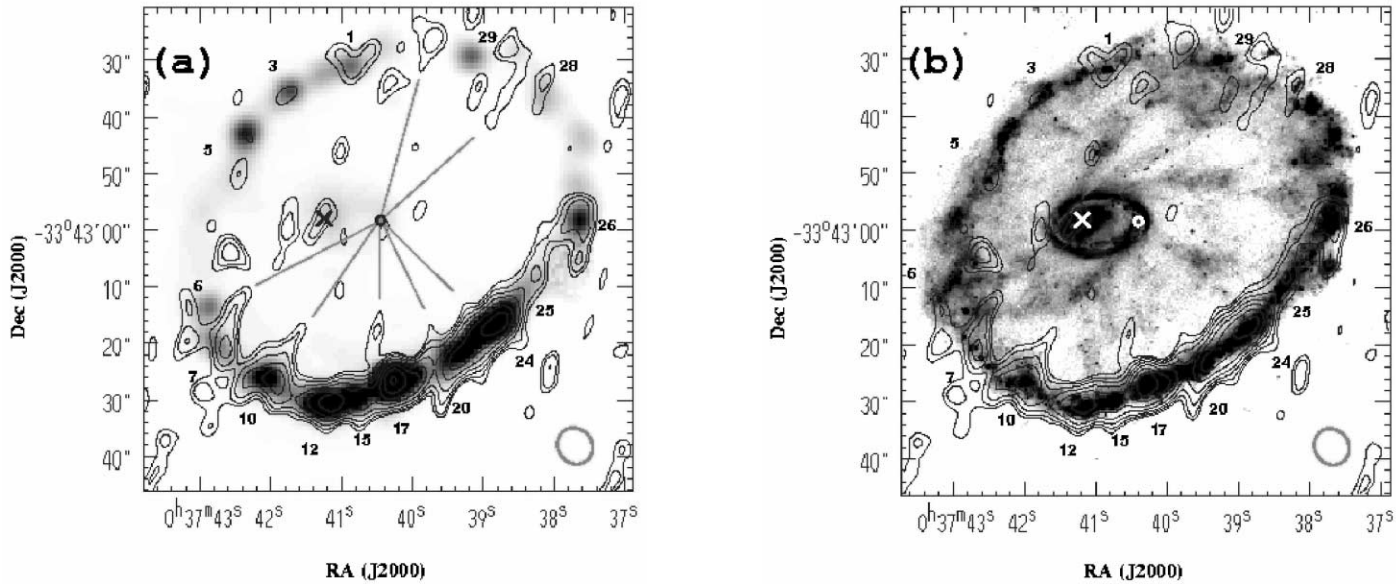

FIG. 1.—The 20 cm RC intensity contours of the Cartwheel superposed on (*a*) an Hα image (*gray scale*), which has been smoothed to the resolution of the 20 cm RC image, and (*b*) the *HST B*-band image. The lowest contour level corresponds to 60 μJy $beam^{-1}$ ($\approx 2\sigma$), and the subsequent contour levels increase by a factor of $\sqrt{2}$. The ellipse at the bottom right corner indicates the RC beam size. In panel *a*, note the excellent positional correspondence between radio peaks and H II complexes, which have been labeled by their H95 numbers. Straight lines are drawn connecting the filamentary structures or spokes to the geometrical center of the ring. Unlike the optical spokes (features connecting the inner ring to the outer ring in panel *b*), the RC spokes are straight and short. The position of the nucleus is marked by a cross. [*See the electronic edition of the Journal for a color version of this figure.*]

first impression from Figure 1*b* is that the relation between the two, if any, is weak. The RC spokes are short and straight, whereas the stellar spokes connect the two rings of the Cartwheel by a curved path. The brightest RC spoke has no correspondence to any optical spoke even when extrapolated inward. Of the other six RC spokes, only one (corresponding to CW-10), when extrapolated inward, meets an optical spoke. On the other hand, some of the weak RC emission interior to the main ring seems to coincide with the brightest points of the stellar spokes. So it is possible that the RC spokes are also longer and curved like their optical counterparts, but we have detected only the bright part of that. Clearly, deeper RC images are required to address this question.

The azimuthal distribution of nonthermal RC intensities and the thermal fraction, in three successive radial zones, one corresponding to the position of the ring (radius = 36″) and the other two positioned 6″ on either side of the ring, are plotted in Figures 2*a*–2*c*. Each zone has a width of 6″. The thermal RC flux is calculated from extinction-corrected Hα flux using the relation given by Condon (1992) for an electron temperature of 15,000 K (Fosbury & Hawarden 1977) and visual extinction $A_v = 1.2$ mag. The azimuthal RC intensity profile of the ring illustrates a well-known fact: regions in the southern part of the ring (P.A. = 120°–240°) are several times brighter than elsewhere in the ring. The spokes stand out in the azimuthal profile of the annular zone in the wake of the ring. The RC emission from the spokes is predominantly nonthermal. The azimuthal profile exterior to the ring resembles that of the ring. However, unlike in the ring where 8%–20% of the observed RC flux of H II complexes is of thermal origin, it is less than 2% in the external zone except for the region just outside CW-12.

3.1. *Global SFR from* Hα*, RC, and FIR Luminosities*

FIR, Hα, and 20 cm RC fluxes have been extensively used as tracers of SFR in galaxies (Kennicutt 1998). The FIR flux, as defined in Condon (1992), is calculated for the Cartwheel using the *IRAS* 60 and 100 μm fluxes from Appleton & Struck-Marcell (1987). The resulting value is given in Table 1, along with the Hα and 20 cm RC flux measured in this work. SFRs are derived from the luminosities in FIR, Hα, and 20 cm RC bands using the relations given by Thronson & Telesco (1986), Kennicutt (1983), and Condon & Yin (1990), respectively. Additive constants that convert log (luminosity) of row 2 to log (SFR) are -9.27, -41.05, and -20.98 for FIR, Hα, and 20 cm RC bands, respectively. The RC conversion factor depends on the nonthermal power-law index α. A value of $\alpha = 0.65$ is used in this work, which is based on the measurement for two of the brightest H II regions in the Cartwheel (H96). In all these relations the initial mass function (IMF) from Kennicutt (1983) was used. Use of Salpeter IMF would decrease the SFRs by 16% (Panuzzo et al. 2003).

In order to calculate the SFR from Hα fluxes, we need to correct for the internal extinction in H II regions. Maximum value of A_v allowed by the observed mean colors of the ring is 1.3 mag (Korchagin et al. 2001), as compared to $A_v = 2.1$ mag measured for the brightest H II region. In the last three rows of Table 1, SFRs are tabulated for $A_v = 0$, 1.2, and 1.7 mag, respectively. FIR-derived SFR is independent of extinction, whereas the SFR derived from nonthermal RC flux is weakly dependent on extinction, which is due to the fact that it is obtained by subtracting the thermal component from the total and that the thermal component is calculated from the extinction-corrected Hα flux. For $A_v = 1.2$ mag, SFR derived from Hα agrees with that from FIR,

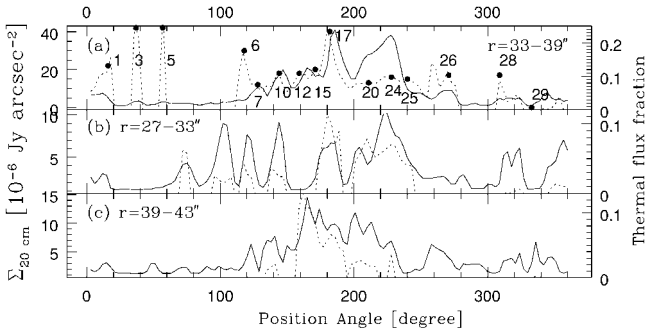

FIG. 2.—Azimuthal profiles of nonthermal RC emission (*solid line*) (*a*) in the ring, (*b*) inside the ring, and (*c*) outside the ring. The thermal fraction at 20 cm is plotted by the dotted line. The brightest 15 H II regions are labeled. Radio continuum spokes are clearly seen in panel *b* at position angles 120°, 145°, 180°, 205°, 225°, 320°, and 355°.

whereas the RC gives around 30% more SFR. The thermal contribution to the global RC flux is 10%, which is in good agreement with the value found for star-forming galaxies (Condon 1992). An SFR of 18 $M_\odot$ yr^{-1} for the Cartwheel compares well with the SFRs of other collisionally formed ring galaxies and interacting galaxies (Marston & Appleton 1995; Dopita et al. 2002).

RC emission of star-forming galaxies is correlated with the FIR emission. Hence, 30% excess SFR derived from RC implies that 30% of the detected RC emission is not related to SF. What is the reason for this excess RC emission in the Cartwheel? A comparison of the RC and Hα morphologies suggests that the regions with excess RC emission are CW-20, CW-24, and the outer boundaries of these regions. Nonthermal radio emission not associated with SF has been discovered in shocked regions in a number of interacting galaxies, including in the intersection of the two merging galaxies forming Antennae (Mazzarella et al. 1988). Considering that the ring in the Cartwheel is expanding at high velocities, it is reasonable to think that the shocked gas contributes to a part of the observed nonthermal RC emission. However, published H I data of the Cartwheel do not show evidence of high velocities suggestive of shocks in these regions. This implies that the neutral gas is not coming from the same region as the shocked ionized gas.

4. DISCUSSIONS

The expanding density wave is expected to leave in its wake old stars and remnants of massive stars. Nonthermal RC emission originates in supernova remnants, which trace stars that are formed ~10–50 Myr ago (lifetime of stars more massive than 9 $M_\odot$ at $Z = Z_\odot/10$). Hence, nonthermal RC emission from spokes represents the trajectory of the star-forming wave over the past ~50 Myr. Intensity distribution along the spokes has valuable information on the past SF process and can be used to constrain the models of SF in an expanding density wave. In Figure 3*a*, we plot the radial profiles of RC and Hα intensities expected from models of SF in an expanding density wave. In particular, we used the Vorobyov & Bizyaev (2001) model, in which the density wave is assumed to be of Gaussian shape $\sigma = 1$ kpc, propagating at 90 km s^{-1} in an exponential gas disk of scale length of 20 kpc. A Schmidt law with power-law index $n = 1.5$ is used to scale gas density to SFR. The RC emission, which traces stars formed ~50 Myr ago, lags behind the Hα peak, which marks the current location of the

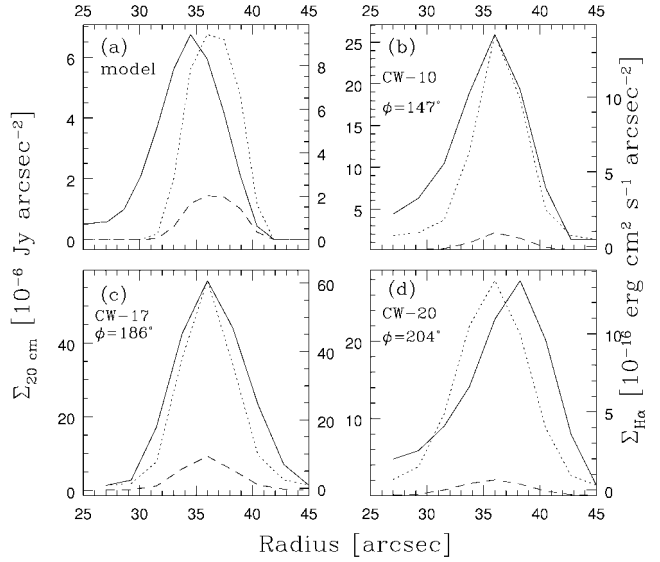

FIG. 3.—Radial intensity cuts along three representative H II complexes compared to a model. The solid lines represent the RC intensities (scale on the left), whereas the dotted lines (scale on the right) denote the intensity of the Hα emission. The dashed lines correspond to the estimated 20 cm thermal component. $A_v = 1.2$ mag is assumed. The H95 identification of the H II regions, as well as the position angle (ϕ) of the regions, are denoted in each panel. Each profile is obtained by averaging in wedges of 3° opening angle.

wave, by about 2″. We have carried out a series of tests and confirmed that the predicted displacements in the peak positions of the profiles should be seen even at the spatial resolution of our RC image.

We obtained radial intensity cuts on the Hα and RC images, passing through the ring center (marked by a small circle in Fig. 1) and the RC detected parts of the ring. All the resulting profiles resemble one of the three representative profiles of Figures 3*b*–3*d*. The majority of the RC profiles are skewed inward as compared to the Hα profile, with the peaks of the two profiles coinciding as in Figure 3*b*. In some directions, the RC emission peaks outside the Hα profile (Fig. 3*c*). RC and Hα profiles of the brightest H II complex (CW-17) are identical except that the former is broader. Surprisingly, none of the regions shows the expected inward shift of the RC profile with respect to Hα profile. The profiles skewed inward correspond to the zones where spokes are detected in the wake of the wave, whereas profiles skewed outward are basically zones where radio emission extends outside the Hα ring. As discussed in the previous section, shocks ahead of the wave are responsible for the RC emission in these zones.

In the Cartwheel, the *K*-band intensity profile, which traces the red supergiant stars that are formed about 10–20 Myr ago, is found to peak marginally inside the Hα profile (Vorobyov & Bizyaev 2003). The displacements are consistent with a wave velocity of ≈100 km s^{-1}. The displacements were not noted along the minor axis cuts, which Vorobyov & Bizyaev (2003) explained as due to orientation effects. H II regions CW-6 and CW-28 are along the major axis, both of which contain radially directed RC spokes, but the expected 2″ shift in the position of peak of the RC emission cannot be noted.

The lack of radial separation between the RC and Hα profiles calls for a revision of the physical ingredients that go into the models, especially in the treatment of SF and feedback effects. The observed profile shapes imply that the SFR increased to the currently observed values abruptly a few tens of Myr ago. A possible reason for the lack of SF in the past could be that the precollisional gas disk was well below criticality and the density enhancements caused by the passing wave were not sufficient to drive the densities above the critical value required for collapse. Even if the disk was critical before the interaction, the passing wave can heat the disk, making it subcritical. Hence, realistic ring models should include heating and cooling of the disk. Observations of more ring galaxies in the RC would be invaluable in working out the details of the physics of SF in an expanding density wave.

We thank the staff at NRAO, especially Barry Clark, for liberal allotment of VLA time. We also thank the staff at McDonald observatory and personally David Doss. This work has gained from discussions with Alessandro Bressan and Vladimir Korchagin at various stages of the project. We thank the anonymous referee whose comments helped to improve the presentation of the manuscript. This work was supported by research grants 39714-F (CONACyT, Mexico), 99-04-OSS-058, and 04-02-16518 (JPL/NASA and RFBR).

REFERENCES

Amram, P., Mendes de Oliveira, C., Boulesteix, J., & Balkowski, C. 1998, A&A, 330, 881
Appleton, P. N., & Struck-Marcell, C. 1987, ApJ, 312, 566
Condon, J. J. 1992, ARA&A, 30, 575
Condon, J. J., & Yin, Q. F. 1990, ApJ, 357, 97
Dopita, M. A., Pereira, M., Kewley, L. J., & Capaccioli, M. 2002, ApJS, 143, 47
Fosbury, R. A. E., & Hawarden, T. G. 1977, MNRAS, 178, 473
Gao, Y., Wang, Q. D., Appleton, P. N., & Lucas, R. A. 2003, ApJ, 596, L171
Gerber, R. A., Lamb, S. A., & Balsara, D. S. 1996, MNRAS, 278, 345
Hamuy, M., Suntzeff, N. B., Heathcote, S. R., Walker, A. R., Gigoux, P., & Phillips, M. M. 1994, PASP, 106, 566
Hernquist, L., & Weil, M. L. 1993, MNRAS, 261, 804
Higdon, J. L. 1995, ApJ, 455, 524 (H95)
Higdon, J. L. 1996, ApJ, 467, 241 (H96)
Kennicutt, R. C., Jr. 1983, ApJ, 272, 54
———. 1998, ARA&A, 36, 189
Korchagin, V., Mayya, Y. D., & Vorobyov, E. I. 2001, ApJ, 554, 281
Lynds, R., & Toomre, A. 1976, ApJ, 209, 382
Marston, A. P., & Appleton, P. N. 1995, AJ, 109, 1002
Mazzarella, J. M., Gaume, R. A., Aller, H. D., & Hughes, P. A. 1988, ApJ, 333, 168
Panuzzo, P., Bressan, A., Granato, G. L., Silva, L., & Danese, L. 2003, A&A, 409, 99
Theys, J. C., & Spiegel, E. A. 1977, ApJ, 212, 616
Thronson, H. A., & Telesco, C. M. 1986, ApJ, 311, 98
Vorobyov, E. I., & Bizyaev, D. 2001, A&A, 377, 835
———. 2003, A&A, 400, 81